Supporting Information

Expanding the limits of amide-triazole isosteric substitution in bisamide-based physical gels

Markus Tautz,[a] Juan Torras,[b,c] Santiago Grijalvo,[d,e] Ramón Eritja,[d,e] César Saldías,[f] Carlos Alemán[b,c] and David Díaz Díaz*[a,g]

[a] *Institut für Organische Chemie, Universität Regensburg, Universitätsstr. 31, 93053 Regensburg, Germany. E-mail: David.Diaz@chemie.uni-regensburg.de*
[b] *Departament d'Enginyeria Química, EEBE, Universitat Politècnica de Catalunya, C/ Eduard Maristany, 10-14, Ed. 12, 08019, Barcelona, Spain*
[c] *Barcelona Research Center for Multiscale Science and Engineering, Universitat Politècnica de Catalunya, C/ Eduard Maristany, 10-14, 08019, Barcelona, Spain*
[d] *Biomedical Research Networking Centre in Bioengineering, Biomaterials and Nanomedicine (CIBER-BBN), Jordi Girona 18-26, 08034 Barcelona, Spain*
[e] *Institute of Advanced Chemistry of Catalonia (IQAC-CSIC), Jordi Girona 18-26, 08034 Barcelona, Spain*
[f] *Departamento de Química Física, Facultad de Química, Pontificia Universidad Católica de Chile, Casilla 302, Correo 22, Santiago, Chile*
[g] *Instituto de Productos Naturales y Agrobiología del CSIC, Avda. Astrofísico Francisco Sánchez 3, 38206 La Laguna, Tenerife, Spain*
E-mail: d.diaz.diaz@ipna.csic.es

Contents List

1. T_{gel} determination

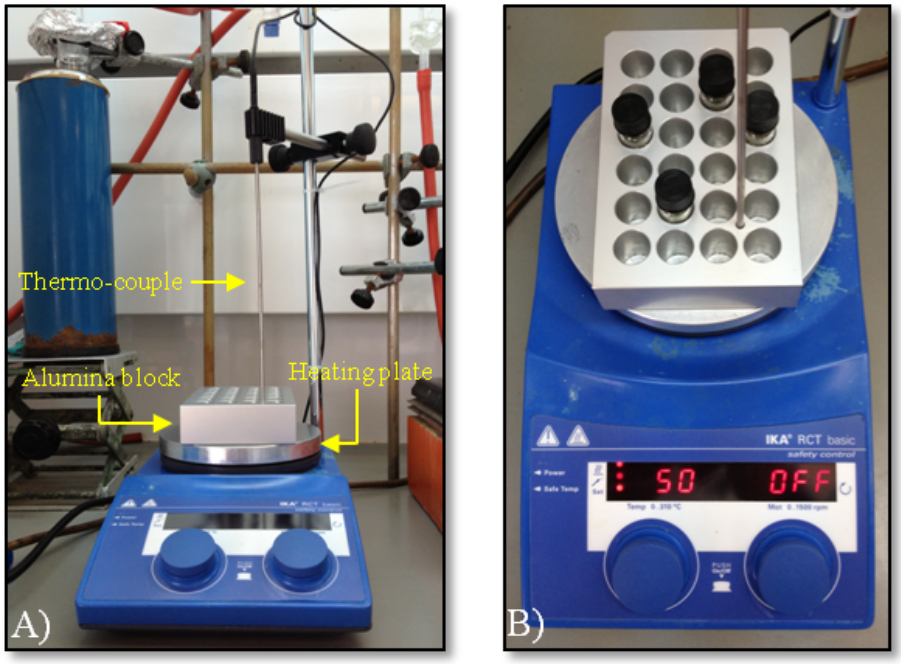

Fig. S1 Custom made set-up for T_{gel} determination. A) Front view showing the composition between electric heating plate, alumina block and digital thermo-couple. B) Top view of the set-up during experimentation containing vials (4 cm length × 1 cm diameter) with gel materials. It is important to mention that the alumina block was constructed especially for one type of vials, which fit smoothly inside the molds to ensure a good transmission of the heat-flow. Verification of the independence of the position inside the custom made apparatus was also performed.

2. Synthesis and characterization of compounds

2.1. Gelator C_{12}-Cyc

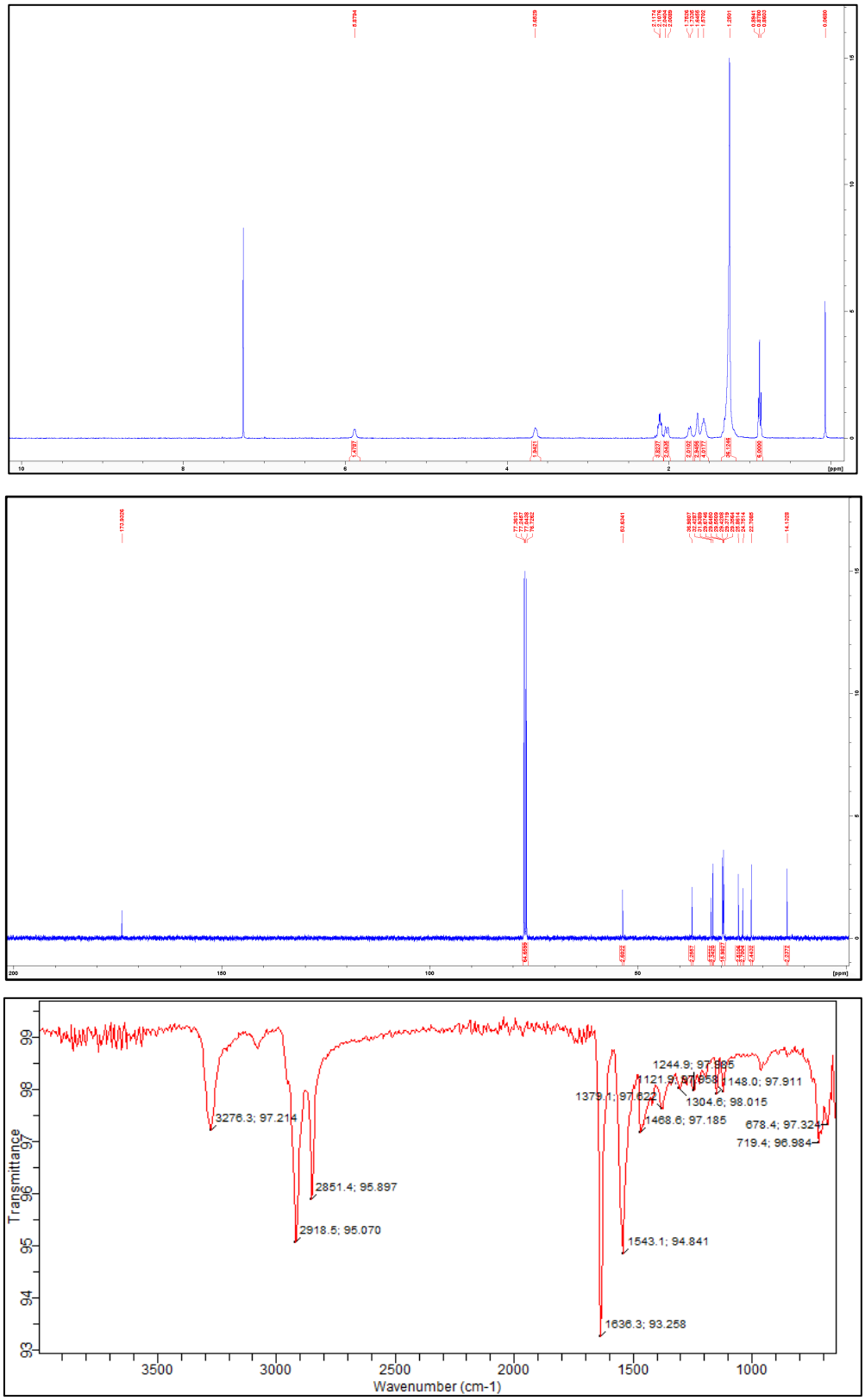

Fig. S2 ^{1}H NMR (*top*), ^{13}C NMR (*middle*), FT-IR (*bottom*) spectra of **C_{12}-Cyc**. NMR spectra were made in $CDCl_3$.

2.2. 1*H*-Imidazole-4-sulfonyl azide (3)

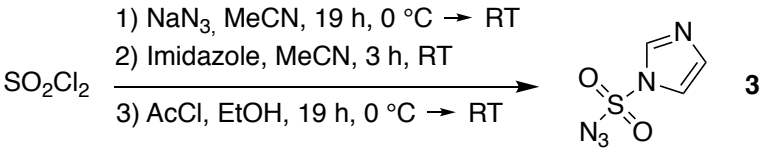

Scheme 1. Synthetic scheme for the preparation of 1*H*-imidazole-4-sulfonyl azide (**3**).

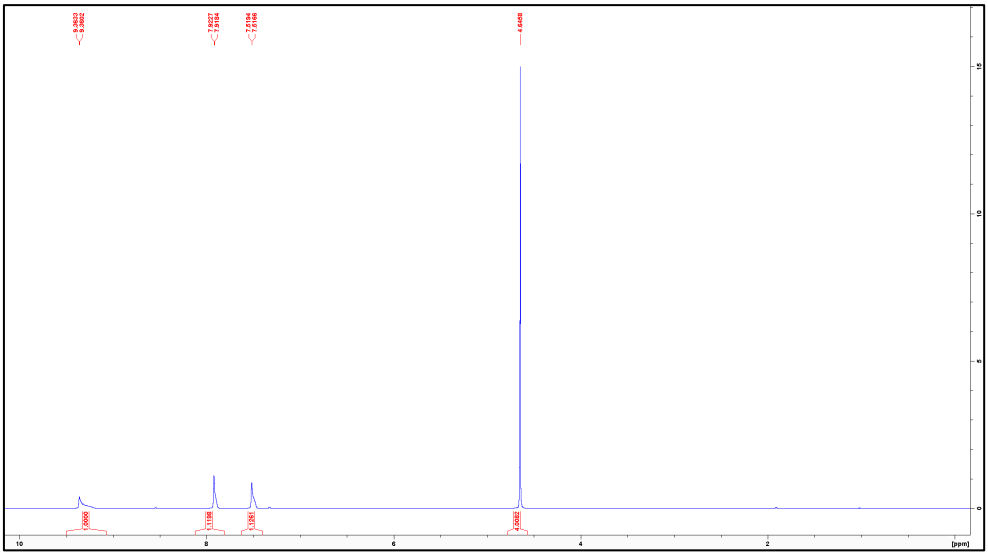

Fig. S3 ^{1}H NMR (D_2O) of reagent **3**.

2.3. (1*S*,2*S*)-1,2-Diazidocyclohexane (4)

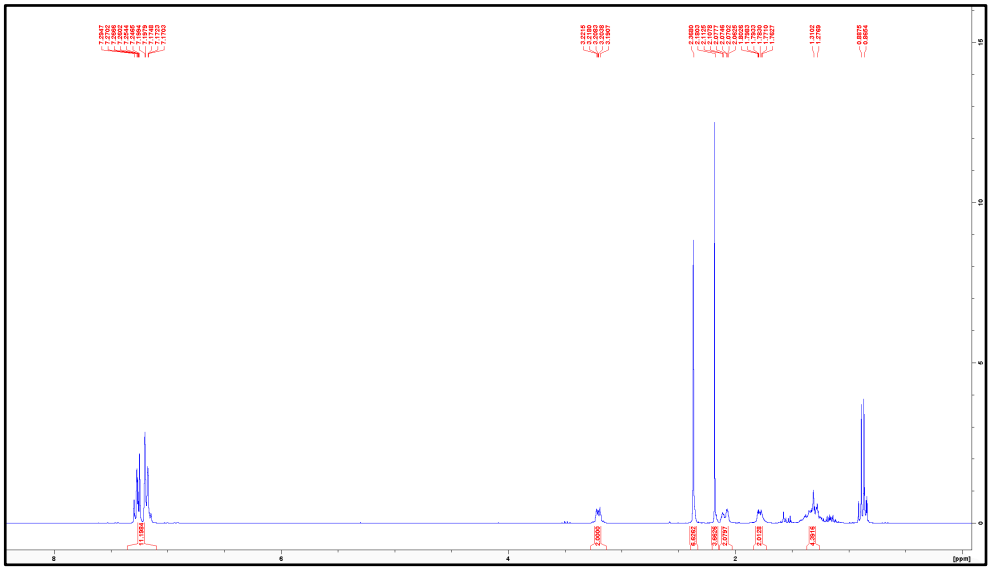

Fig. S4 ^{1}H NMR ($CDCl_3$) spectrum of diazide **4**.

2.4. Gelator click-C_{12}-Cyc

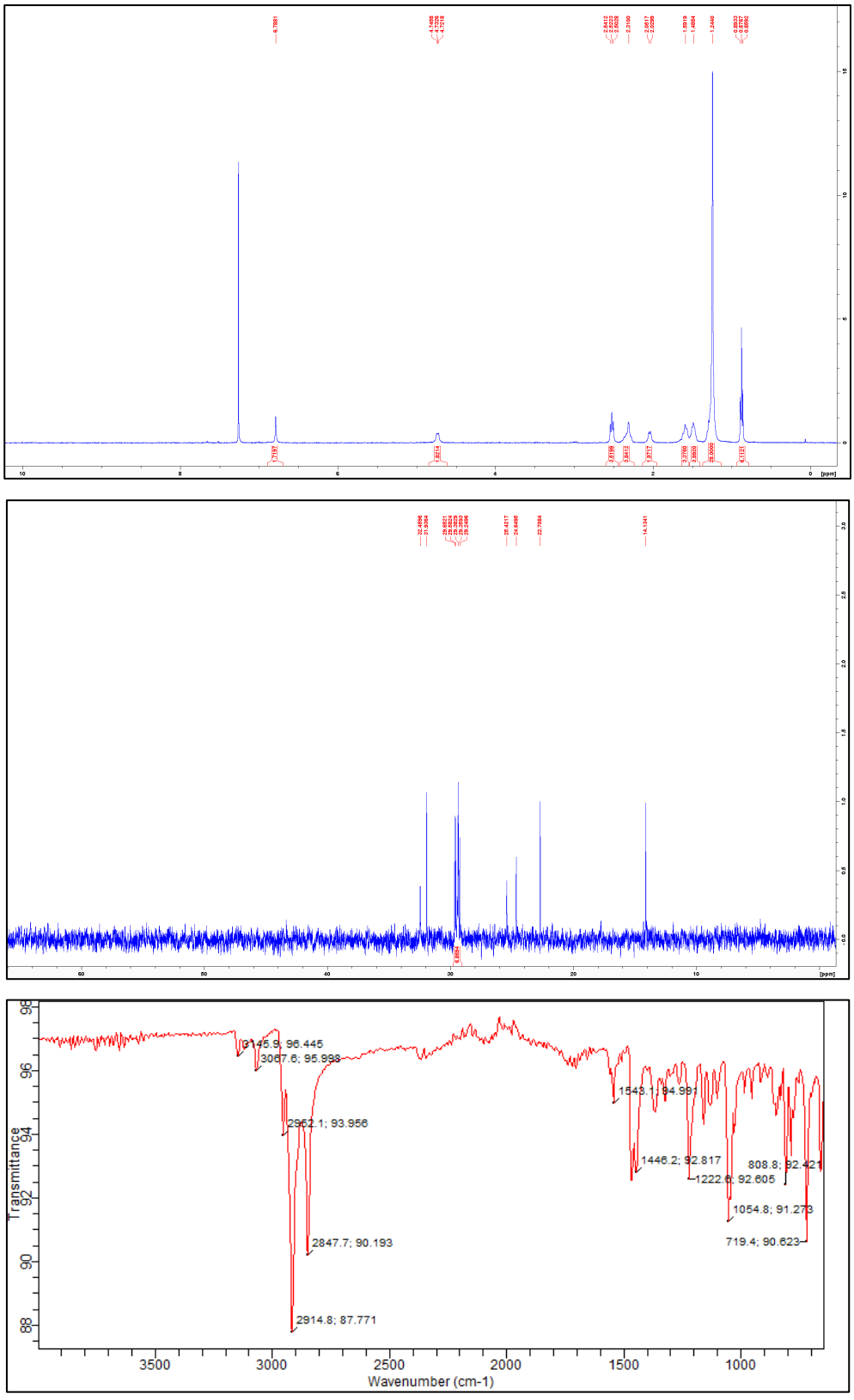

Fig. S5 ^{1}H NMR (*top*), ^{13}C NMR (*middle*) and FT-IR (*bottom*) spectra of **click-C_{12}-Cyc**. NMR spectra were made in $CDCl_3$.

2.5. Click-C_{13}-Cyc

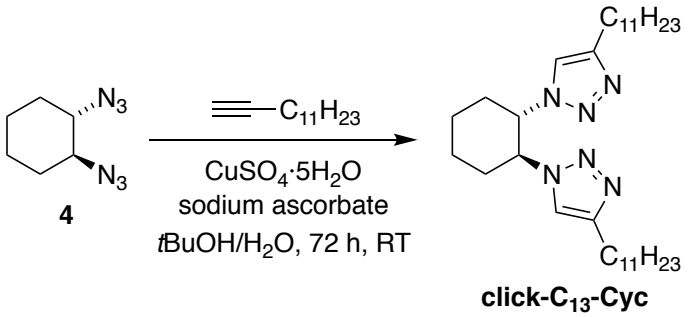

Scheme 2. Synthetic scheme for the preparation of (1*S*,2*S*)-1,2-bis(4-undecyl-1*H*-1,2,3-triazol-1-yl)cyclohexane (**click-C_{13}-Cyc**).

Click-C_{13}-Cyc was prepared following the exact same route as during the synthesis of **click-C_{12}-Cyc**, using1-tridecyne (2.1 equiv) instead of 1-dodecyne. **Click-C_{13}-Cyc** was obtained as a light yellow solid in 49% yield (124 mg, 0.235 mmol). M.p. 121 ºC; ^{1}H NMR (400 MHz, $CDCl_3$) δ (ppm) 6.85 (s, 2H), 4.77 (m, 2H), 2.55 (m, 4H), 2.32 (m, 4H), 2.05 (m, 2H), 1.60 (m, 2H), 1.50 (m, 4H), 1.25 (s, 32H), 0.88 (t, J = 6.64 Hz, 6H); ^{13}C NMR (101 MHz, $CDCl_3$) δ (ppm) 64.07, 32.40, 29.70, 29.66, 29.58, 29.45, 29.48, 29.24, 25.48, 24.63, 22.71, 14.14; FT-IR (ATR) ν_{max} (cm^{-1}) 3146, 3116, 3068, 2956, 2919, 2751, 1703, 1543, 1469, 1375, 1223, 1055, 850, 805, 723; MS (ESI): *m/z* = 264.2 $[M+2H]^{2+}$, 527.5 $[M+H]^{+}$. Elemental analysis calculated for $C_{30}H_{54}N_6$: C, 72.95; H, 11.10; N, 15.95; found: C, 71.73; H, 10.70; N, 15.12. The enantiomer (*i.e.* (1*R*,2*R*)-1,2-bis(4-undecyl-1*H*-1,2,3-triazol-1-yl)cyclohexane) was prepared following the same route using (1*R*,2*R*)-1,2-diaminocyclohexane as starting material.

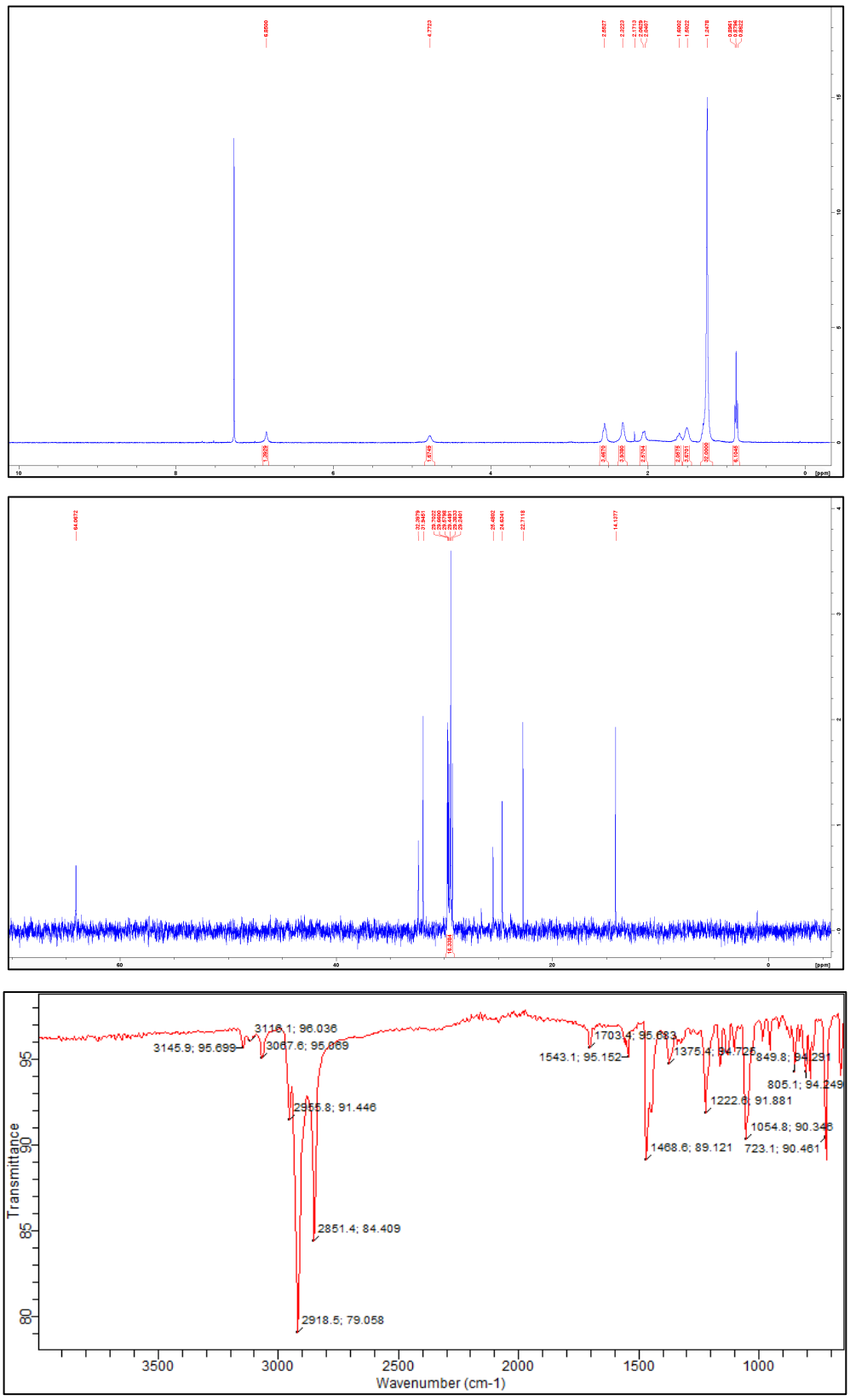

Fig. S6 ^{1}H NMR (*top*), ^{13}C NMR (*middle*) and FT-IR (*bottom*) spectra of **click-C_{13}-Cyc**. NMR spectra were made in $CDCl_3$.

3. Tabular data of gelation ability and gel properties

Table S1 Comparison of gelation ability and typical gel properties of **C_{12}-Cyc** and **click-C_{12}-Cyc** in various organic solvents.[a]

Solvent	**C_{12}-Cyc**				**click-C_{12}-Cyc**			
	CGC ($g\ L^{-1}$)	Gelation time (min)	T_{gel} (°C)	Appearance	CGC ($g\ L^{-1}$)	Gelation time (min)	T_{gel} (°C)	Appearance
Cyclohexane	11[b]	2.0 ± 0.5	51 ± 2	OG	14 ± 1	11 ± 2	34 ± 2	OG
Ethylene glycol	4.5 ± 0.5	2.5 ± 0.5	53 ± 5	OG	16 ± 2	0.2 ± 0.1	48 ± 2	OG
Gasoline	5 ± 0.5	1.0 ± 0.25	75 ± 5	OG	9 ± 1	2 ± 0.5	47 ± 4	OG
Hexane	6[b]	0.1[c]	58 ± 3	OG	33 ± 3[d]	0.1[c]	56 ± 5	OG
Liquid paraffin	4 ± 0.5	1.2 ± 0.1	43 ± 4	TLG	3 ± 0.5	4 ± 1	52 ± 6	TLG
Methanol	20[b]	15 / 0.5[c]	39 ± 1	CR	36 ± 2	1.0 ± 0.5[c]	38 ± 2	CR
Nitromethane	3 ± 0.5	1.0 ± 0.1	50 ± 2	OG	18 ± 4	1.5 ± 0.2	47 ± 1	OG
PTFE oil	8 ± 1	3 ± 0.5	58 ± 2	OG	22 ± 3	4.4 ± 0.2	44 ± 3	OG
Silicone oil	2[b]	7 ± 1	51 ± 2	TLG	1.4 ± 0.2	50 ± 5	46 ± 2	TLG

[a] Error values reported as STDV were estimated from at least two randomized experiments. [b] From ref. 23 (main text). [c] Ultrasound sonication of the isotropic solution was necessary. [d] Gelator precipitated at lower concentrations. Abbreviations: OG = opaque gel; TLG = translucent gel; CR = crystalline appearance.

Table S2 CGCs for gels made of **C_{12}-Cyc**, **click-C_{12}-Cyc** and **click-C_{13}-Cyc** in all tested solvents.[a]

Solvent	**C_{12}-Cyc**	**click-C_{12}-Cyc**	**click-C_{13}-Cyc**
	CGC (g L^{-1})	CGC (g L^{-1})	CGC (g L^{-1})
2-Methylbutan-2-ol	85 ± 5	-[c]	-[c]
2-Methylpentan-1-ol	40 ± 5	-[c]	-[c]
2-Methylpropan-1-ol	-[c]	-[c]	-[c]
2-Methylpropan-2-ol	29 ± 2	-[c]	-[c]
Acetone	10[b]	-[c]	21 ± 3
Acetonitrile	5[b]	-[c]	26 ± 5
Benzene	20[b]	-[c]	-[c]
Butan-1-ol	53 ± 3	-[c]	-[c]
Butan-2-ol	34 ± 3	-[c]	-[c]
Butane-1,4-diol	2 ± 0.5	-[c]	-[c]
Cyclohexane	11[b]	14 ± 1	32 ± 2
Decan-1-ol	38 ± 4	-[c]	-[c]
Diethyl ether	3 ± 0.5	-[c]	-[c]
Dimethyl sulfoxide	4 ± 1	-[c]	5 ± 1
Dodecan-1-ol	31 ± 2	-[c]	-[c]
Ethanol	33[b]	-[c]	26 ± 3
Ethyl acetate	8[b]	-[c]	-[c]
Ethylene glycol	4.5 ± 0.5	16 ± 2	11 ± 3
Glycerole	-[d]	-[e]	-[e]
Gasoline	5 ± 0.5	9 ± 1	37 ± 4
Heptan-1-ol	34 ± 3	-[c]	-[c]
Hexan-1-ol	43 ± 4	-[c]	-[c]
Hexane	6[b]	33 ± 3[f]	37 ± 4
Liquid paraffin	4 ± 0.5	3 ± 0.5	-[c]
Methanol	20[b]	36 ± 2	37 ± 4
N,N-Dimethylacetamide	11[b]	-[c]	16 ± 3
N,N-Dimethylformamide	10[b]	-[c]	21 ± 3
Nitromethane	3 ± 0.5	18 ± 4	16 ± 3
N-Methyl-2-pyrrolidone	17 ± 3	-[c]	16 ± 3
Nonan-1-ol	34 ± 4	-[c]	-[c]
Octan-1-ol	43 ± 4	58 ± 4	68 ± 5
Pentan-1-ol	43 ± 4	-[c]	-[c]
Pentan-2-ol	15 ± 2	-[c]	-[c]
Pentane-1,5-diol	3 ± 0.5	-[c]	-[c]
Propan-1-ol	44[b]	-[c]	63 ± 4
Propan-2-ol	40[b]	-[c]	21 ± 3
PTFE oil	8 ± 1	22 ± 3	21 ± 3
Pyridine	25[b]	-[c]	32 ± 4
Silicone oil	2[b]	1.4 ± 0.2	13 ± 2
Undecan-1-ol	38 ± 4	-[c]	-[c]
Water	-[d]	-[e]	-[e]

[a] Error values reported as STDV were estimated from at least two randomized experiments. [b] From ref. 23 (main text). [c] Precipitation of the gelator was observed after cooling down the isotropic solution. [d] Gelator remained insoluble. [e] Gelator formed a solid layer on top of solvent after cooling down the isotropic solution. [f] Precipitation of gelator took place at concentrations below the CGC. Note: None of the gelators were unable to selectively gel the organic solvent in monophasic mixtures of DMSO or EtOH and water.

4. CD spectroscopy

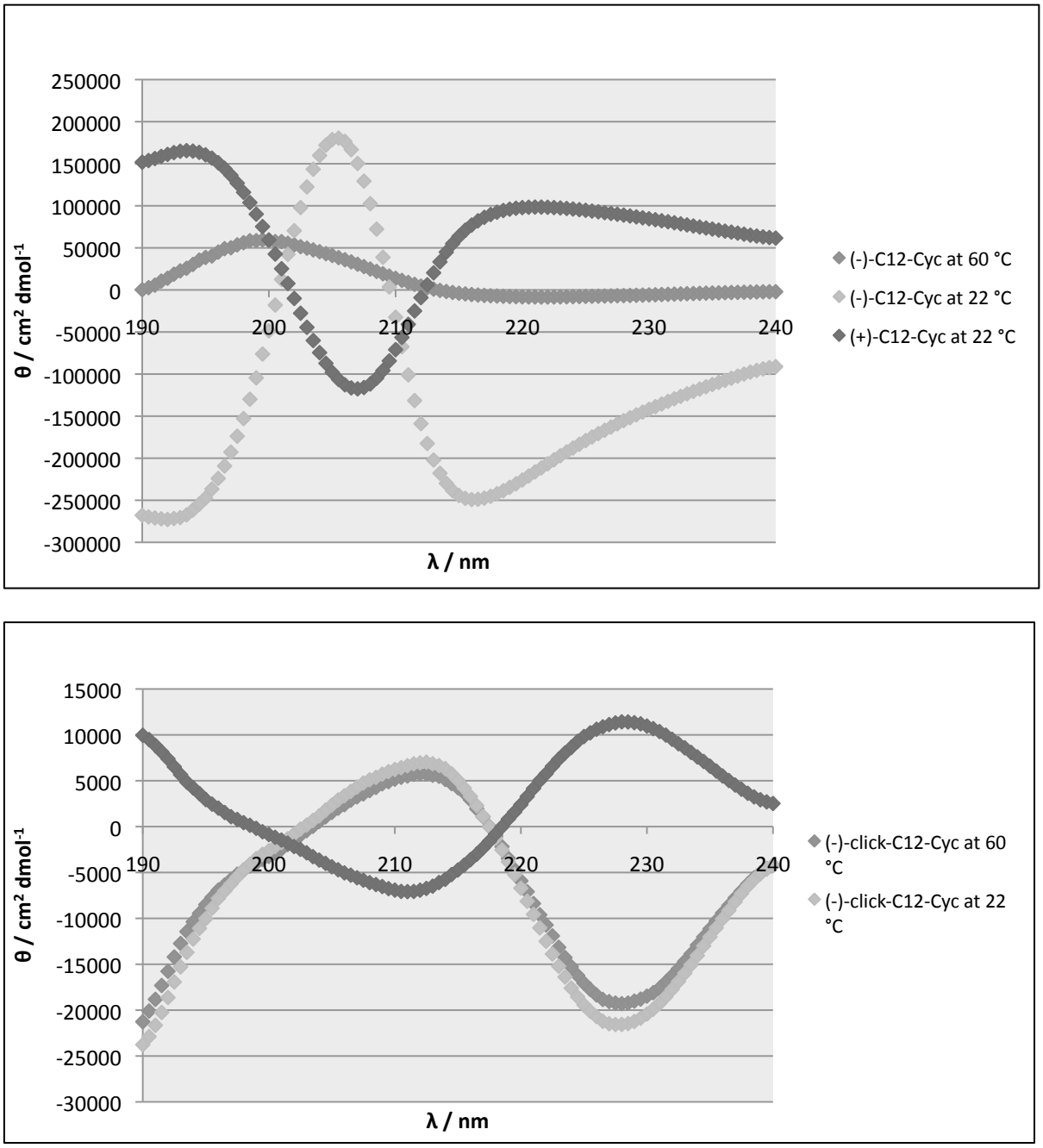

Fig. S7 CD spectra of **C_{12}-Cyc** gels in acetonitrile (c = 1 mmol L^{-1}) (*top*) and **click-C_{12}-Cyc** solutions in acetonitrile (c = 1 mmol L^{-1}) (*bottom*). Note: As the gelators were measured at concentrations of 1 mmol L^{-1} in acetonitrile due to intense scattering at higher concentrations, **click-C_{12}-Cyc** didn't form a gel under these conditions at 22 °C leading to a much lower molar ellipticity, as well as a disappearing temperature dependency of the aggregate's stereo information. As expected and in agreement with previous studies, the ellipticity of **C_{12}-Cyc** measured at 60 ºC decreased drastically due to the thermal *gel*-to-*sol* transition, in concordance with the origin of the CD bands from a chiral aggregate of the gelator. However, **click-C_{12}-Cyc** gave the same results as when measured at 22 °C. The CD peaks were found to be long-wave shifted for **click-C_{12}-Cyc**.

5. Effect of gelator concentration on T_{gel} and gelation kinetics

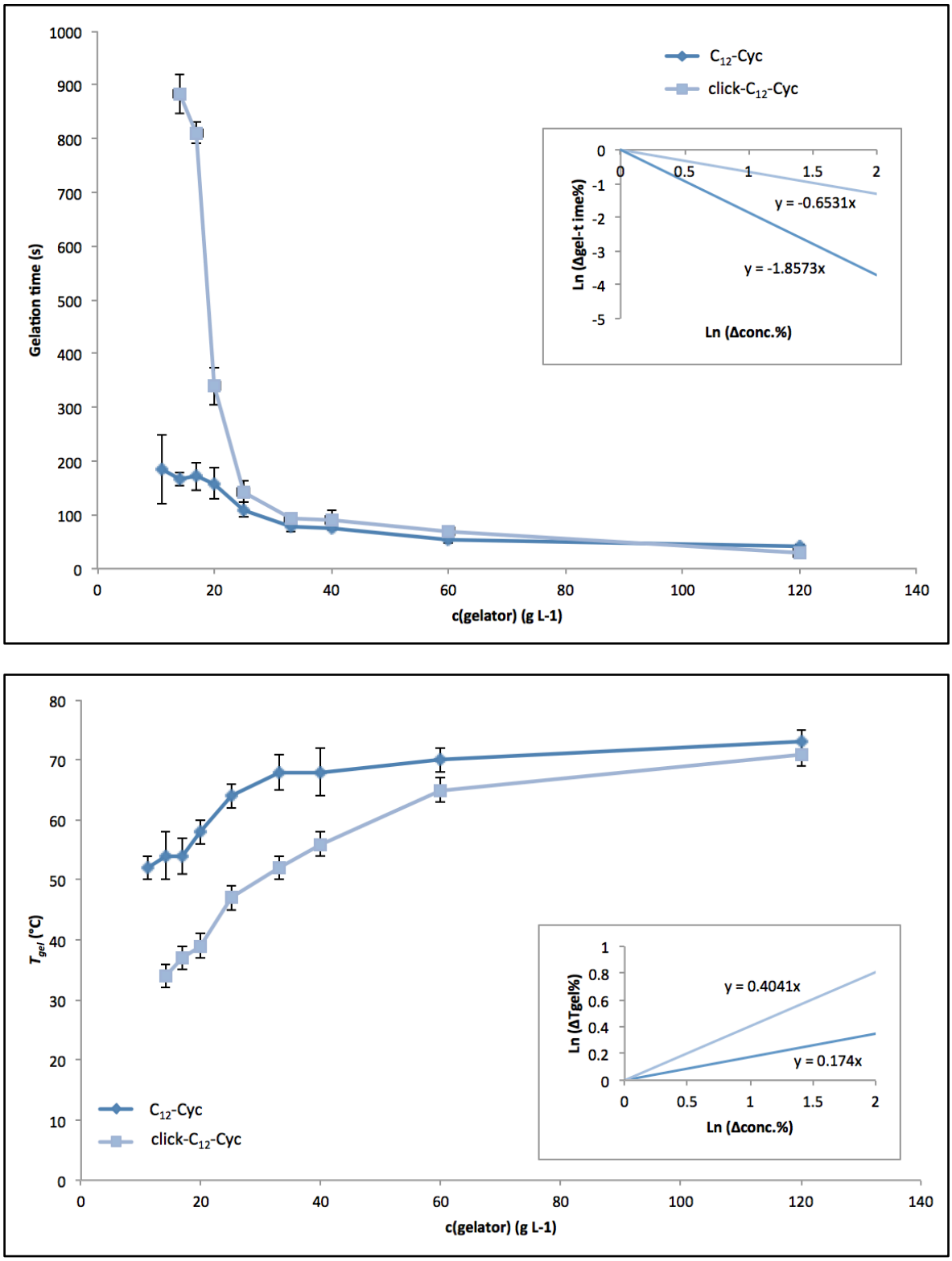

Fig. S8 Evolution of T_{gel} with increasing gelator concentration of gels made from **C_{12}-Cyc** (*top*) and **click-C_{12}-Cyc** (*bottom*) in cyclohexane. Inset-plots: Normalized Ln-Ln plots of the corresponding percentual increments. Note: In general, all gelators showed very quick gelation kinetics in the range of few seconds to 1 h and showed full thermo-reversibility except for the gels formed in hexane and methanol, which relied on sonication to enable reversible gelation.

6. Additional electron microscopy images

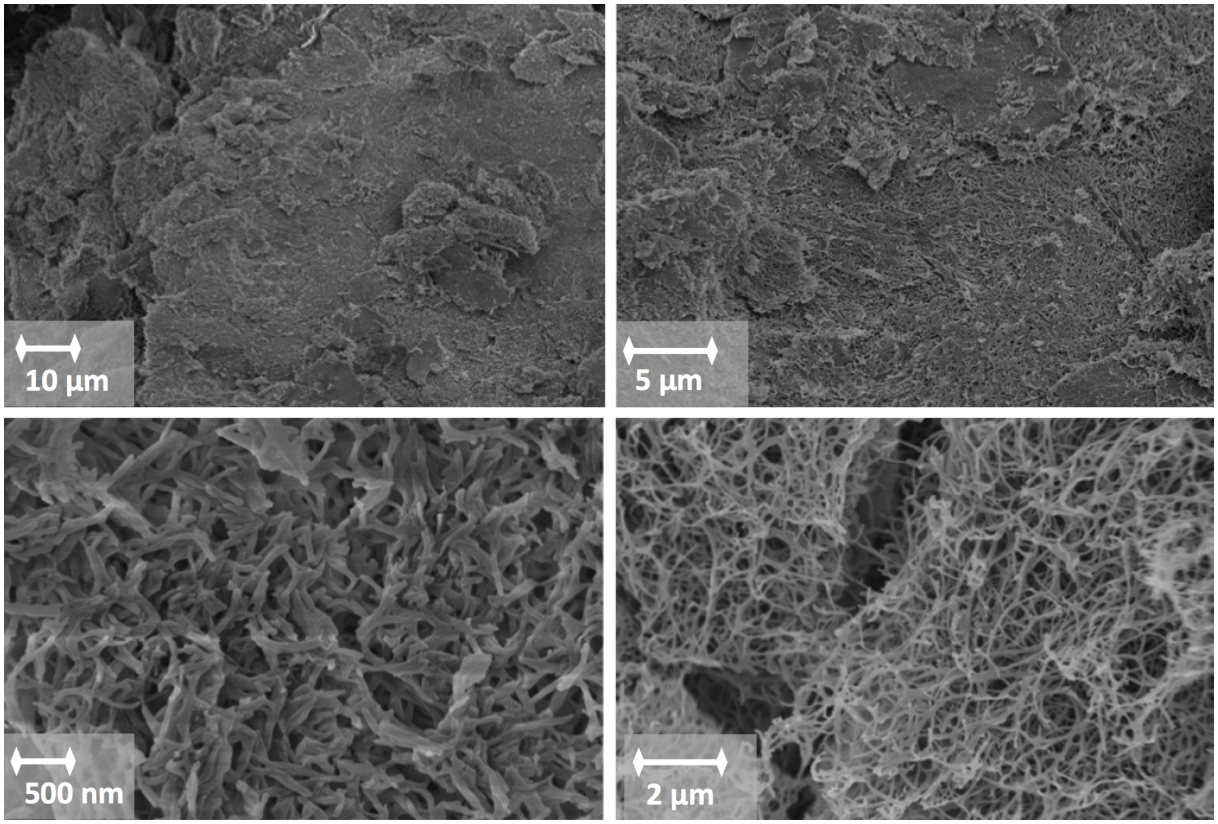

Fig. S9 Additional FESEM pictures of a xerogel prepared from **C_{12}-Cyc** (c = 20 g L^{-1}) in cyclohexane.

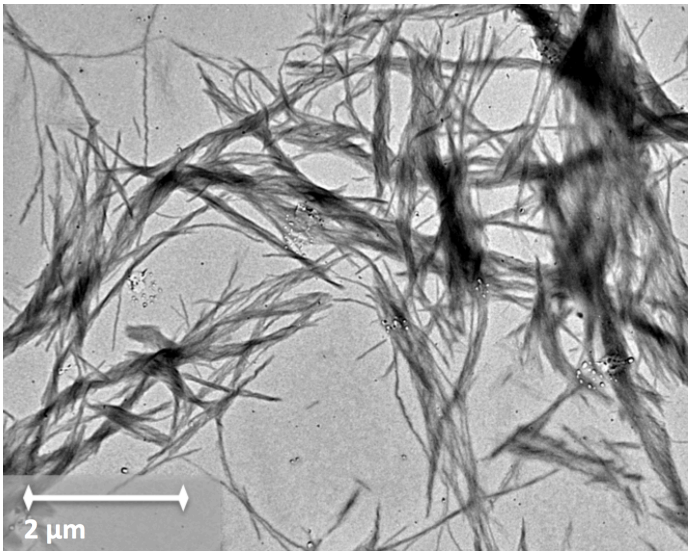

Fig. S10 Representative TEM image of the gel made of **C_{12}-Cyc** (c = 20 g L^{-1}) in cyclohexane.

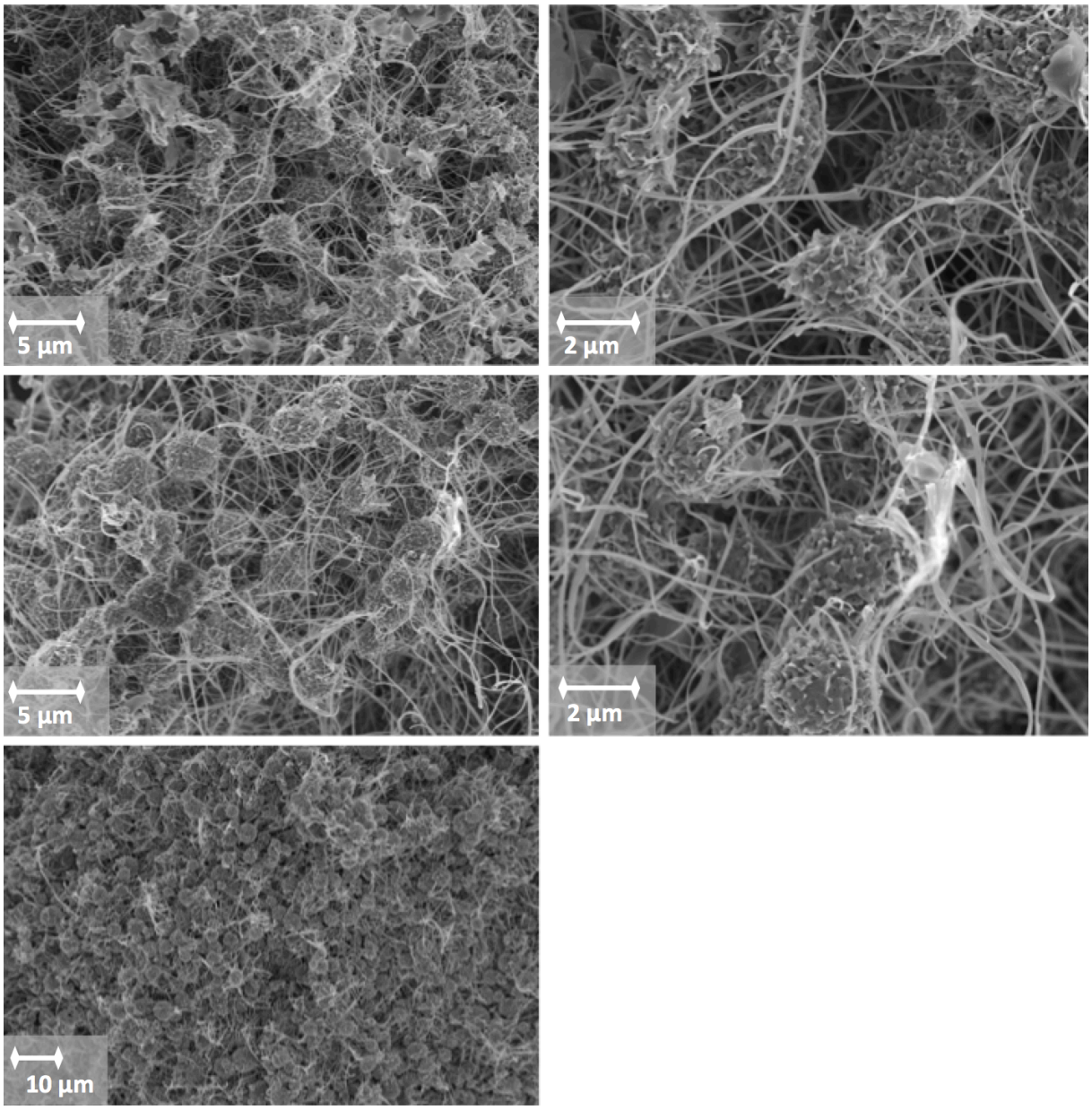

Fig. S11 Additional FESEM pictures of a xerogel prepared from **click-C_{12}-Cyc** (c = 20 g L^{-1}) in cyclohexane.

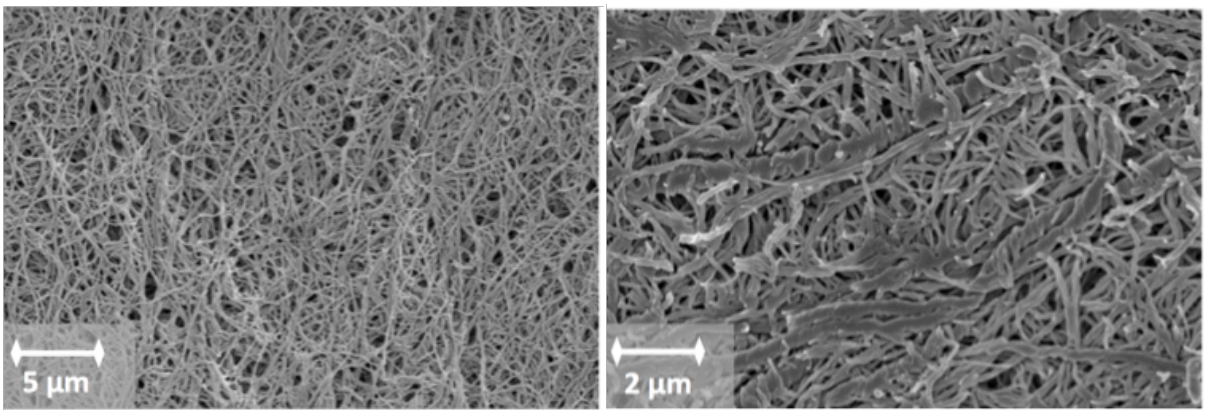

Fig. S12 Additional FESEM pictures of a xerogel prepared from **C_{12}-Cyc** (c = 30 g L^{-1}) in nitromethane.

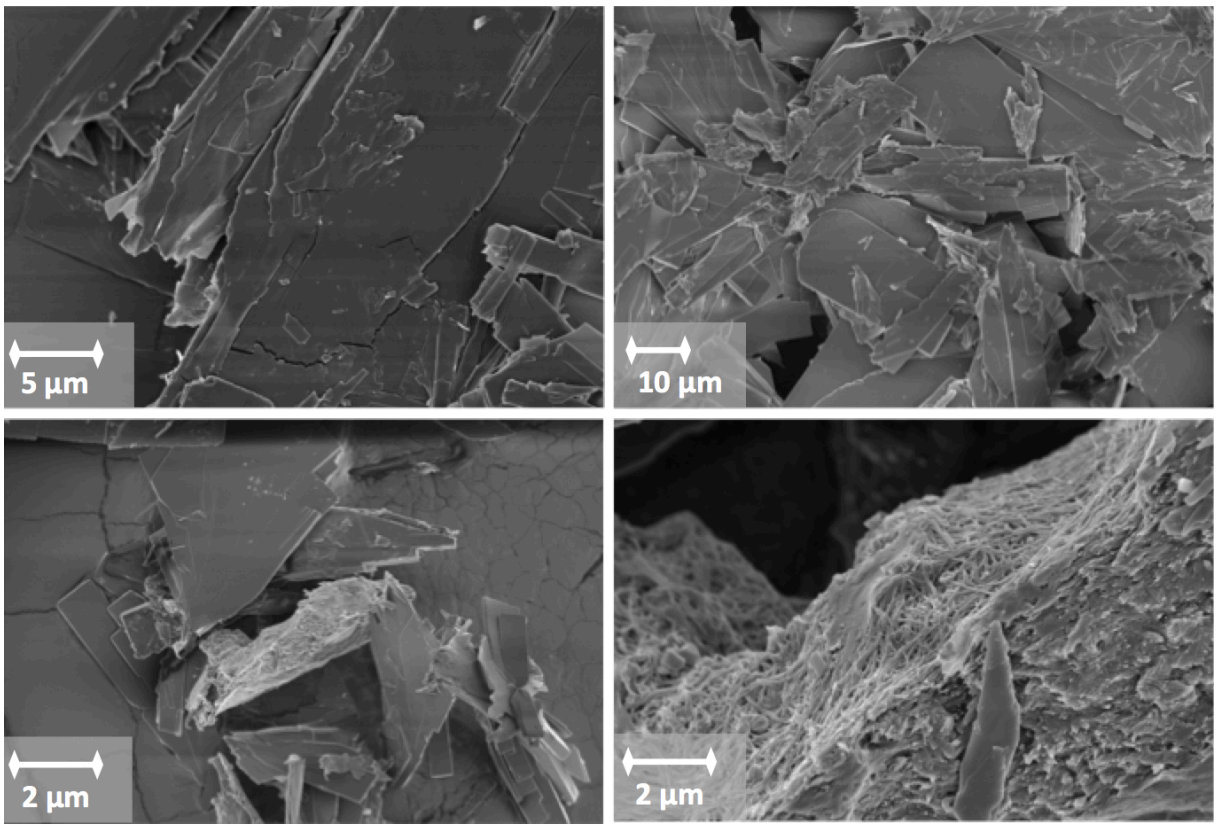

Fig. S13 Additional FESEM pictures of a xerogel prepared from **click-C_{12}-Cyc** (c = 30 g L^{-1}) in nitromethane.

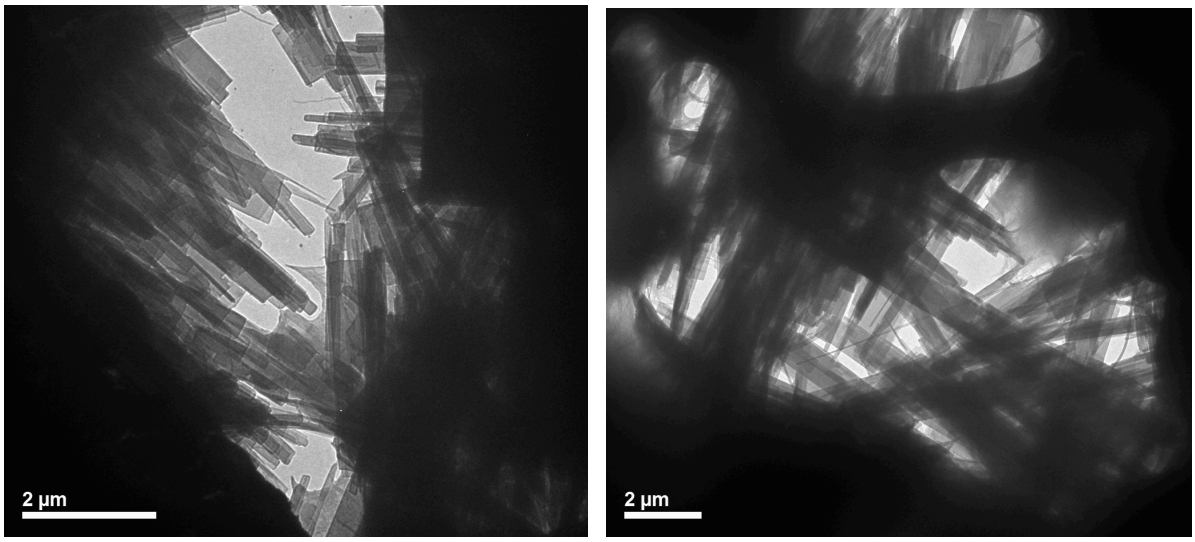

Fig. S14 Representative TEM images of gels made of **click-C_{12}-Cyc** (c = 30 g L^{-1}) in nitromethane.

7. Rheological measurements

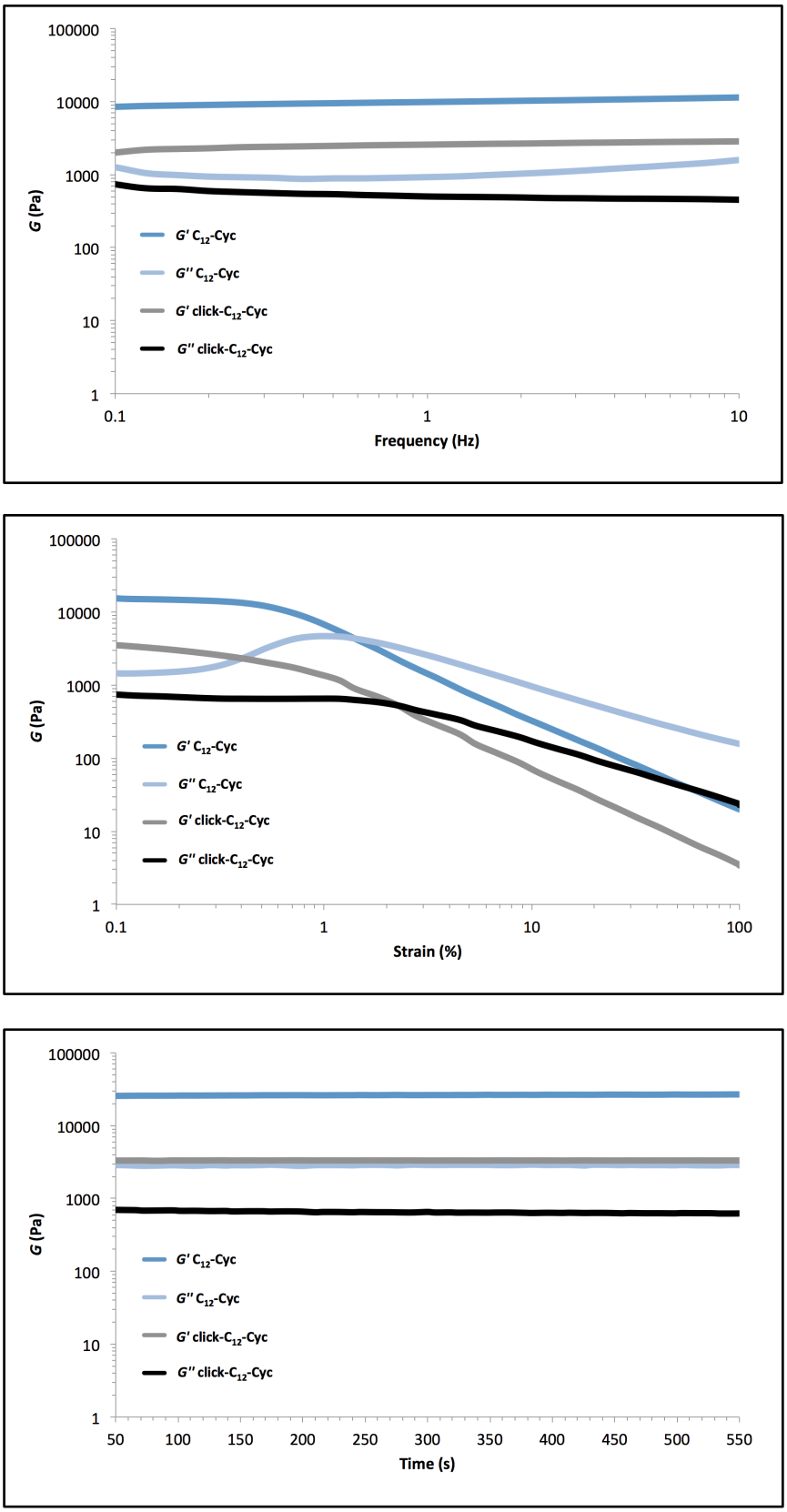

Fig. S16 Oscillatory rheological experiments of gels prepared from **C_{12}-Cyc** and **click-C_{12}-Cyc** in cyclohexane (c = 20 g L^{-1}). *Top*: DFS-plots. *Middle*: DSS-plots. *Bottom*: DTS-Plots.

8. Cytotoxicity studies

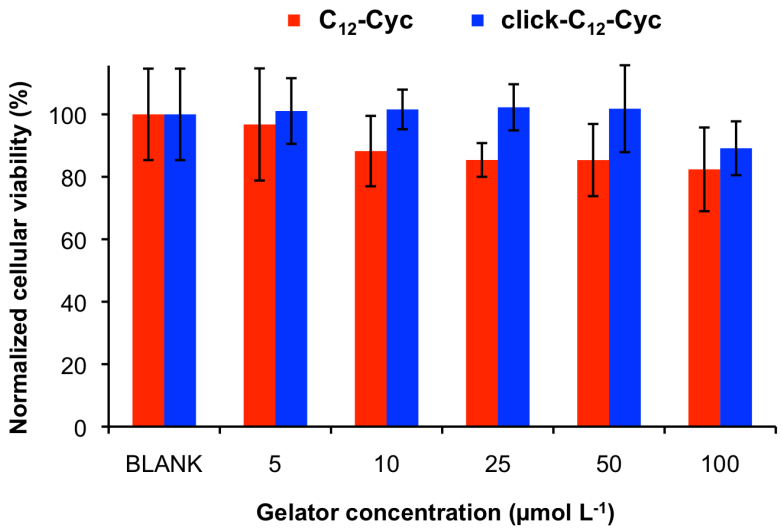

Fig. S16 *In vitro* cytotoxicity activities of the synthesized gelators **C_{12}-Cyc** and **click-C_{12}-Cyc** at different concentrations (5, 10, 25, 50 and 100 μM). Toxicities were evaluated according to the MTT assay using untreated HeLa cells as a control (Blank). Both gelators were incubated in the presence of HeLa cells for 24 hours at 37 ºC. Cellular viabilities were significant at 10 μM ($^{*}\rho < 0.05$) and 25 μM ($^{**}\rho < 0.01$).

Table S3 Tabular data of cytotoxicity studies. Average values and errors were determined in at least 6 randomized entries for each experiment.

	C_{12}-Cyc	**click-C_{12}-Cyc**
c (gelator) (μmol L^{-1})	Normalized cellular viability (%)	Normalized cellular viability (%)
0	100 ± 15	100 ± 15
5	97 ± 18	101 ± 11
10	88 ± 11	102 ± 6
25	85 ± 5	102 ± 7
50	85 ± 11	102 ± 14
100	82 ± 13	89 ± 9

9. FT-IR spectroscopy of xerogels

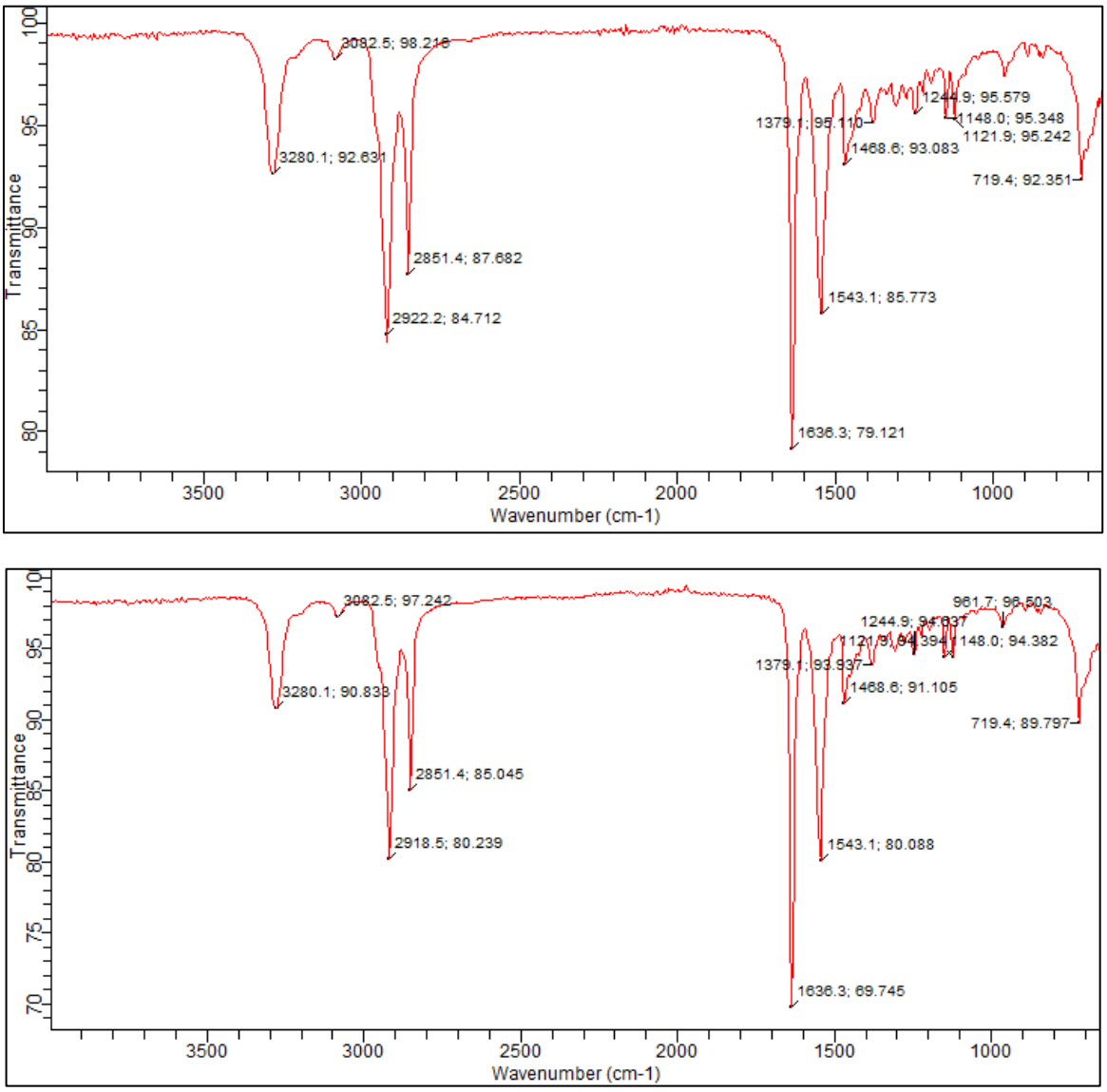

Fig. S17 FT-IR spectra of **C_{12}-Cyc** xerogel in cyclohexane (c = 15 g L^{-1}) (*top*) and **C_{12}-Cyc** xerogel in nitromethane (c = 20 g L^{-1}) (*bottom*).

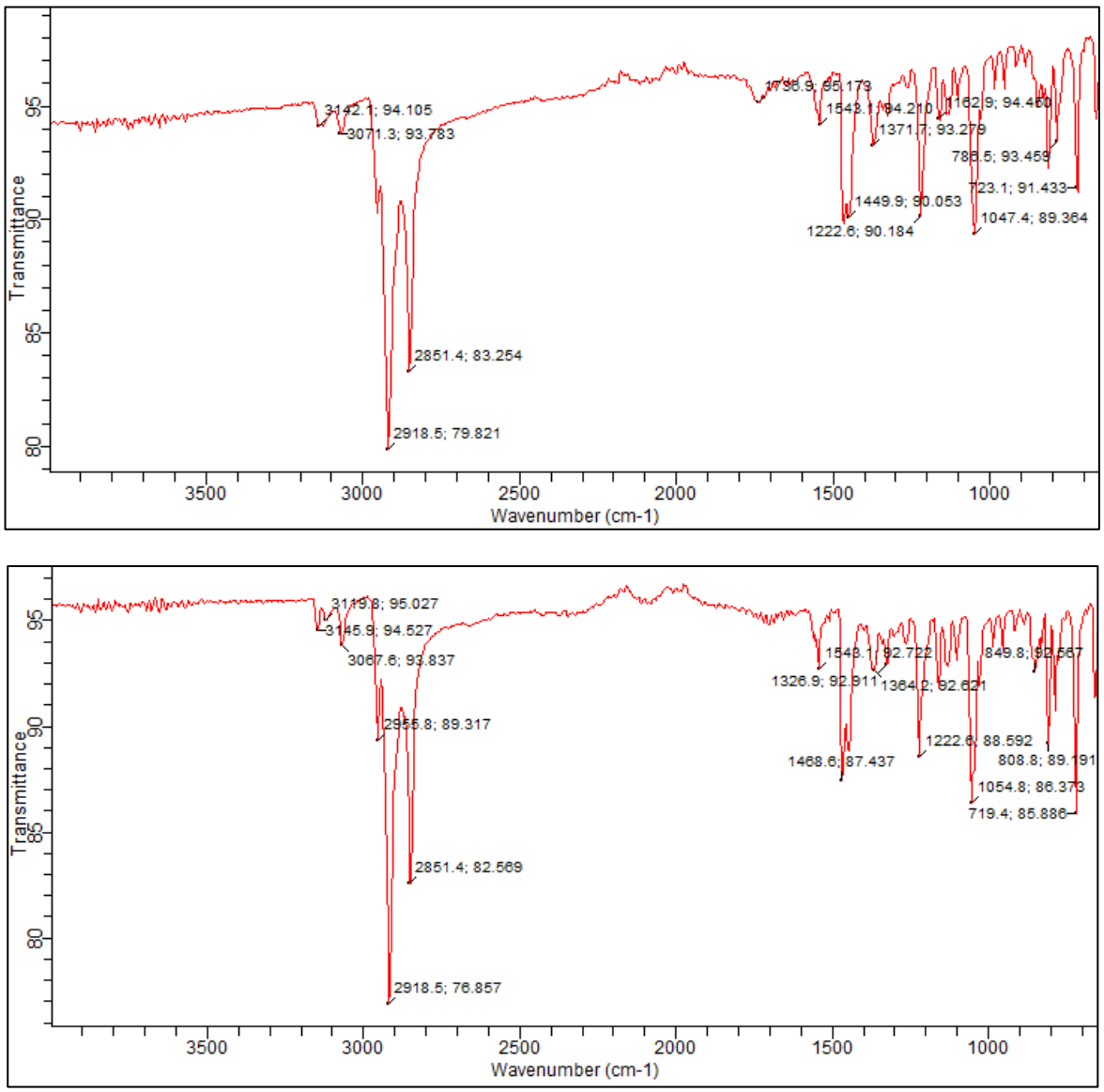

Fig. S18 FT-IR spectra of **click-C_{12}-Cyc** xerogel in cyclohexane (c = 15 g L^{-1}) (*top*) and **click-C_{12}-Cyc** xerogel in nitromethane (c = 20 g L^{-1}) (*bottom*).

10. XRD spectroscopy

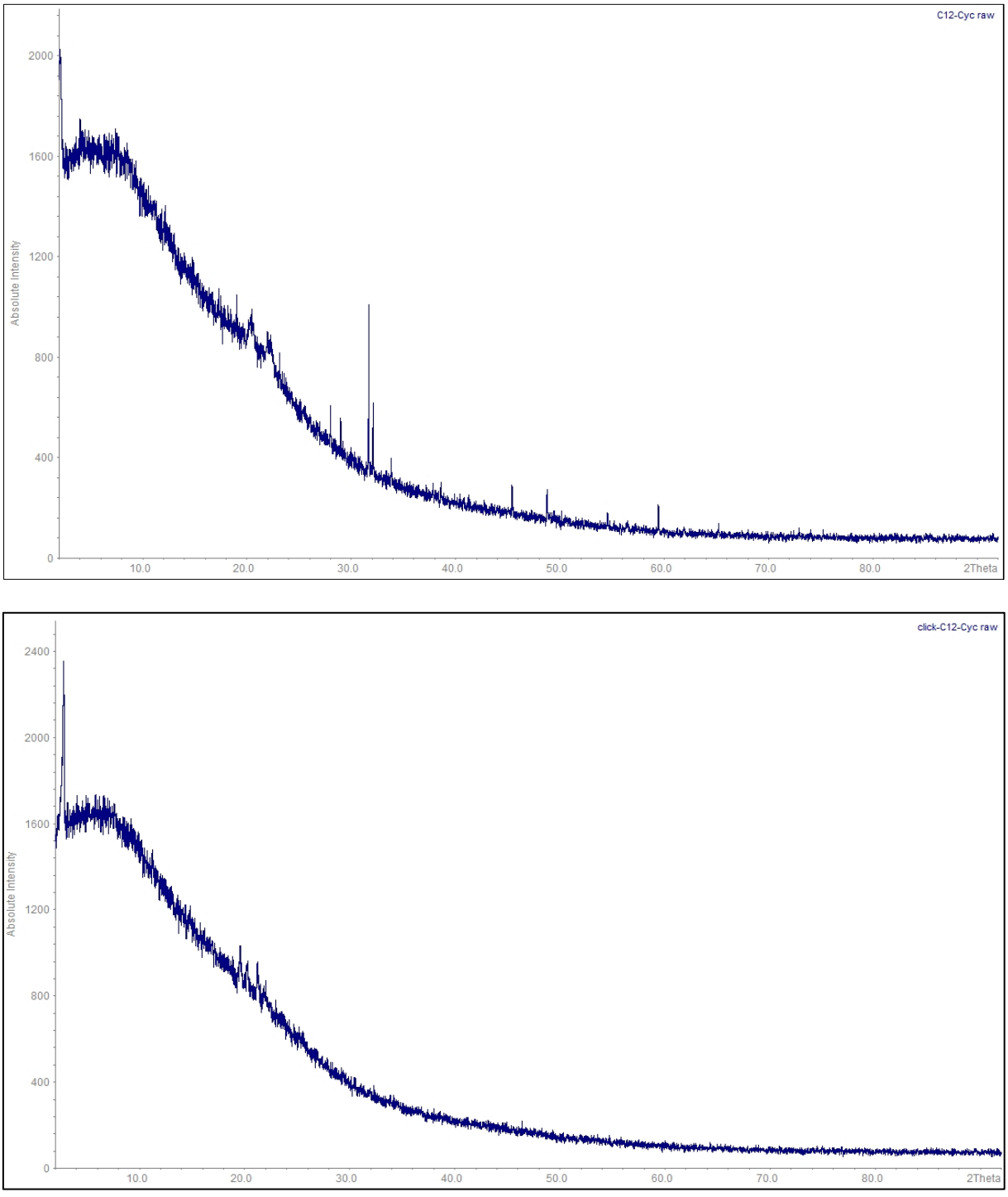

Fig. S19 XRD spectra of raw **C_{12}-Cyc** (*top*) and raw **click-C_{12}-Cyc** (*bottom*) as the compounds were recrystalized from acetone during the synthesis.

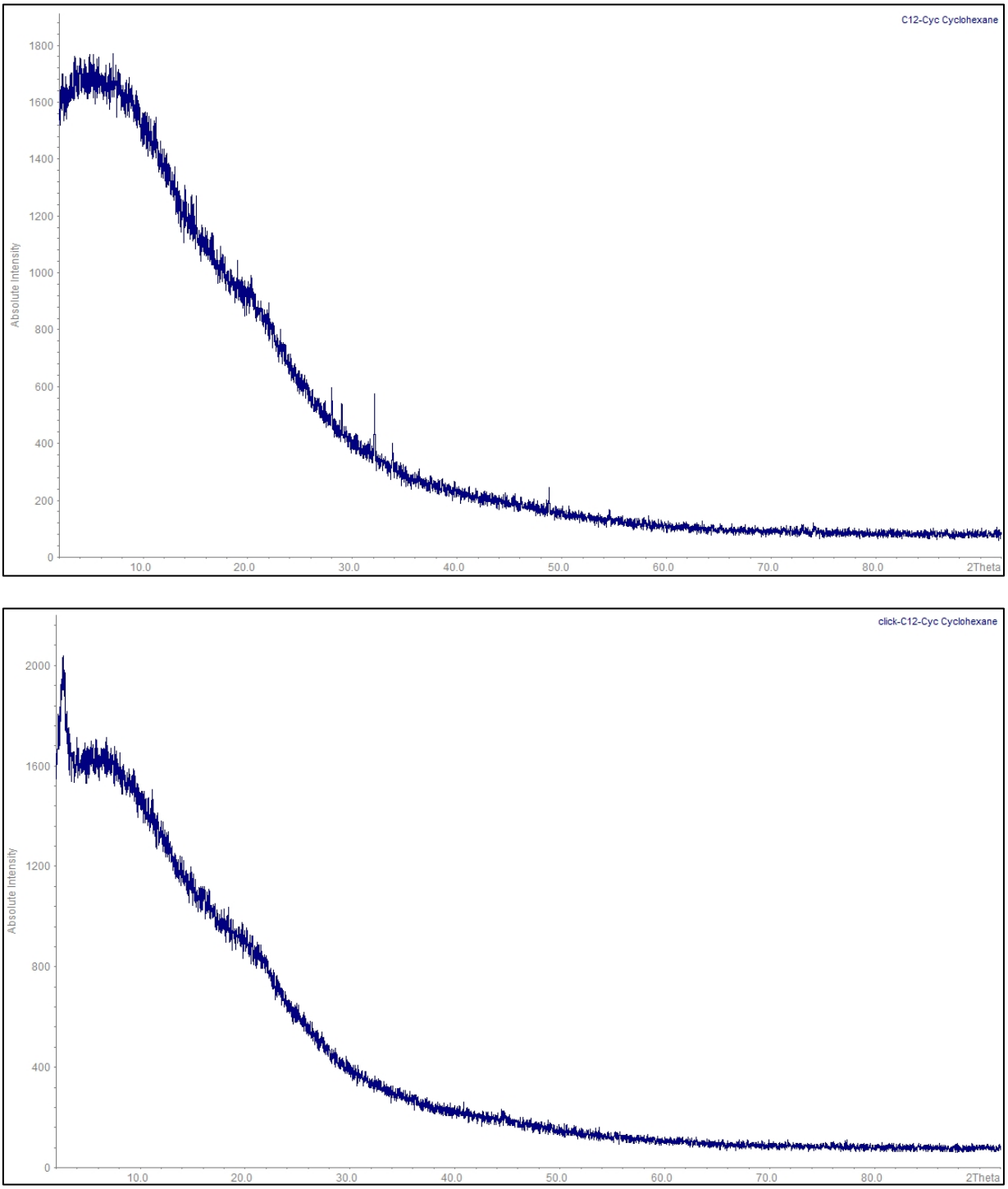

Fig. S20 XRD spectra of **C_{12}-Cyc** (c = 15 g L^{-1}) (*top*) and **click-C_{12}-Cyc** (c = 15 g L^{-1}) (*bottom*) xerogels in cyclohexane.

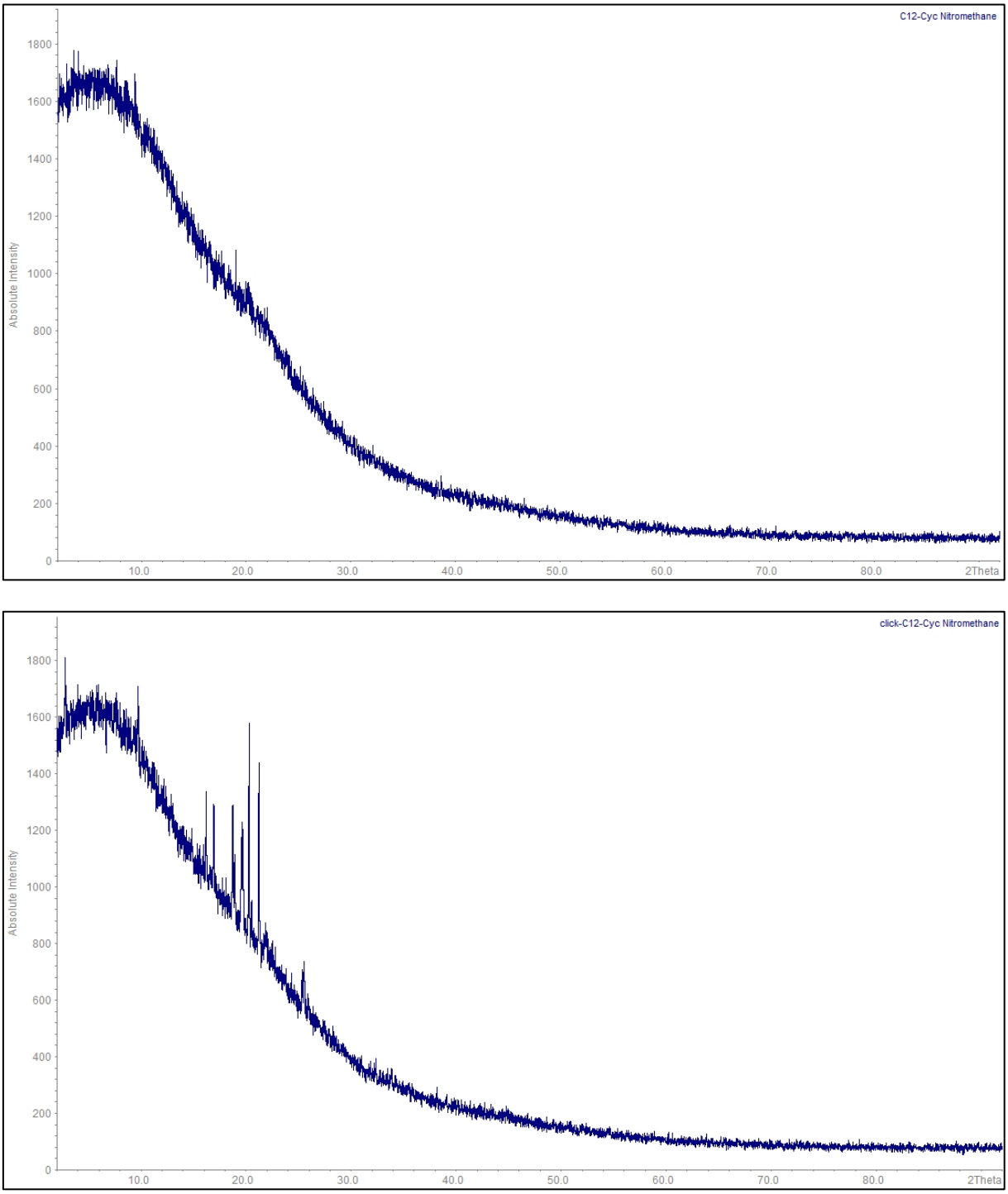

Fig. S21 XRD spectra of **C_{12}-Cyc** (c = 20 g L^{-1}) (*top*) and **click-C_{12}-Cyc** (c = 20 g L^{-1}) (*bottom*) xerogels in nitromethane.

11. Computational studies

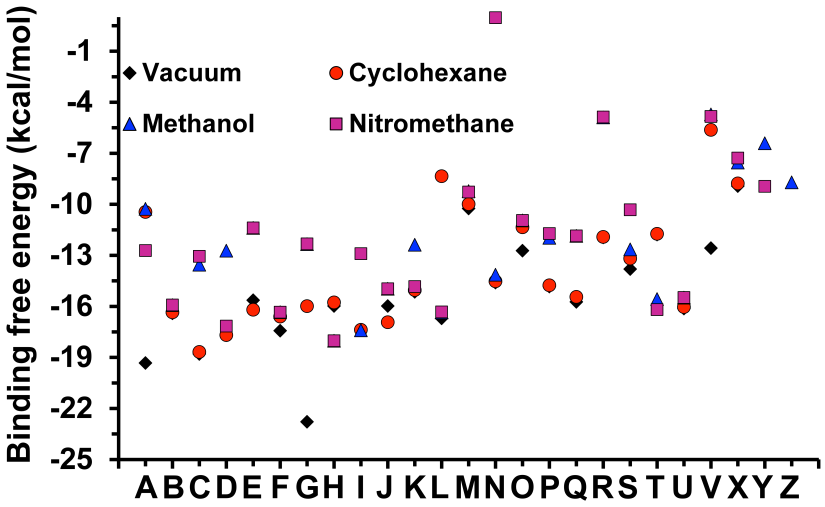

Fig. S22 Binding free energy of model complexes calculation in vacuum, cyclohexane, methanol and nitromethane. Complexes have been labeled from A to Z, each letter referring to the complex optimized using the same starting point for each environment.